

# Contact Conductance of Selected Metal–Matrix Composites

D. G. Blanchard\* and L. S. Fletcher†

Texas A&M University, College Station, Texas 77843-3123

Thermal contact conductance data are reported for metal–matrix composite materials at various temperatures. The surfaces were ground using a diamond wheel; therefore, the surface characterization parameters were anisotropic. The measurements were for 2124 aluminum with silicon carbide particulate ( $\text{SiC}_p$ ) volumetric loading fractions of 25 and 30%, and 6061 aluminum with  $\text{SiC}_p$  loading fractions of 40 and 55%. The results were nondimensionalized and compared with a recent contact conductance theory that accounts for surface slope anisotropy of conforming rough surfaces. All data were consistently overpredicted by the theory, which does not include composite material effects. In fact, the sample surfaces did not show the bivariate normal surface slope distribution fundamentally assumed by the theory. It was concluded that a new theory may be needed to account for composite particle effects, surface slope distributions other than bivariate normal, or both of these effects.

## Nomenclature

$H_c$	= contact microhardness
$h_c$	= contact conductance
$k_s$	= harmonic mean thermal conductivity
$m_0$	= surface height variance
$m_{2\min}$	= minimum profile slope variance
$m_{2\max}$	= maximum profile slope variance
$P$	= apparent contact pressure
$\nu$	= ratio of minimum to maximum rms profile slopes

## Subscript

$p$  = particulate

## Introduction

THE utilization of metal–matrix composite materials (MMCs) has steadily increased due to the maturation of fabrication technology over the last two decades for these novel materials. One fabrication methodology utilizes metal and silicon carbide powder that is mixed and hot-pressed. This process allows various properties of the material to be selectively controlled by varying the percentage of silicon carbide particulate ( $\text{SiC}_p$ ). These “isotropic powder metallurgy” materials typically find applications where dimensional stability control is required, as a result of their capability for coefficient of thermal expansion tailoring. Thermal contact conductance has been measured extensively for many metals using similar and dissimilar interface materials.<sup>1</sup> To a lesser extent, investigators have also made thermal contact conductance measurements on composite materials.<sup>2–4</sup> These measurements have been primarily on graphite fiber–epoxy systems. The present investigation provides contact conductance data for aluminum alloy matrix materials reinforced with particulate silicon carbide, and compares the results with the theoretical model of DeVaal et al.<sup>5</sup> for conforming rough surfaces with surface slope anisotropy. Interface temperatures varied between 268–376 K. Detailed Vickers microhardness

data and surface topography measurements were made for all contacting surfaces.

## Literature Review

Mohn and Vukobratovich<sup>6</sup> described four successful design applications using MMC materials. The MMC system components described were 1) an instrument cover for a missile inertial measurement unit, 2) gimbal components for an imaging infrared guidance system, 3) mirror substrates for optical systems, and 4) an ultralightweight telescope. Two values of thermal conductivity were given in the paper, both at an unspecified temperature. For instrument grade 6061-T6 40 vol % particulate  $\text{SiC}$ , 127 W/m-K (74 Btu/h-ft-F) was reported. For optical grade 2124-T6 30 vol % particulate  $\text{SiC}$ , the value was 123 W/m-K (72 Btu/h-ft-F).

Both Rubin<sup>7</sup> and Kinner<sup>8</sup> have written overview articles on the applications of MMCs. The applications listed included jet engine fan blades, satellite, missile, and helicopter parts, storage battery plates, antennae structures, superconductor restraints in fusion power reactors, electrical contacts and bearings, and high-temperature structures.

In 1987, DeVaal et al.<sup>5</sup> developed a method for predicting the contact conductance of conforming rough surfaces that contain surface slope anisotropy. The model described the surface slope directional variations with a bivariate normal probability distribution. Elliptical contact areas were assumed whose average major and minor axis ratio was seen to be equivalent to the ratio of the minimum and maximum rms asperity slope. The resulting thermomechanical contact conductance model yielded the following nondimensional expression that correlated the results for the range  $(1.0 \times 10^{-5} < P/H < 2.0 \times 10^{-2})$  and  $(0.1 < \nu < 1.0)$ :

$$\frac{h_c \sqrt{m_0}}{k_s (\sqrt{m_{2\max}} \sqrt{m_{2\min}})^{1/2}} = \left( 0.986 - \frac{0.0075}{\nu} \right) \left[ \frac{P}{H_c} \right]^{[0.95 - (0.004/\nu)]}$$

In 1989, Yovanovich and Nho<sup>9</sup> described experimental contact conductance results of ground and lapped stainless steel 304 surfaces. The dependence of contact conductance on mean interface temperature was experimentally verified. Experimental results were compared to the isotropic model of Cooper et al.<sup>10</sup> and the anisotropic model of DeVaal et al.<sup>5</sup> Results indicated that the best agreement between theory and the experimental data was obtained by using measured surface slope data at 45 deg to the lay, and accounting for the effect of temperature on the contact microhardness.

Presented as Paper 92-2847 at the AIAA 27th Thermophysics Conference, Nashville, TN, July 6–9, 1992; received Jan. 26, 1993; revision received Oct. 30, 1994; accepted for publication Nov. 12, 1994. Copyright © 1994 by the American Institute of Aeronautics and Astronautics, Inc. All rights reserved.

\*Graduate Research Assistant, Department of Mechanical Engineering; currently at Naval Air Warfare Center, China Lake, CA. Member AIAA.

†Thomas A. Dietz Professor, Department of Mechanical Engineering. Fellow AIAA.

Table 1 Metal matrix composites surface characteristics

Material	Vickers microhardness, kg/mm <sup>2</sup>	Surface	Roughness	Asperity slope	Surface	Waviness
		rms, $\mu\text{m}$	Arithmetic mean, $\mu\text{m}$	rms	rms, $\mu\text{m}$	Arithmetic mean, $\mu\text{m}$
25% SiC <sub>p</sub> , 2124 aluminum	210	0.565 $\pm$ 0.060	0.422 $\pm$ 0.034	0.131 $\pm$ 0.012	1.108 $\pm$ 0.365	0.909 $\pm$ 0.282
		0.556 $\pm$ 0.055	0.419 $\pm$ 0.033	0.109 $\pm$ 0.012	1.131 $\pm$ 0.339	0.950 $\pm$ 0.302
		0.303 $\pm$ 0.059	0.240 $\pm$ 0.045	0.067 $\pm$ 0.011	1.093 $\pm$ 0.489	0.893 $\pm$ 0.435
30% SiC <sub>p</sub> , 2124 aluminum	243	0.864 $\pm$ 0.034	0.690 $\pm$ 0.028	0.387 $\pm$ 0.098	1.300 $\pm$ 0.461	1.021 $\pm$ 0.350
		0.653 $\pm$ 0.042	0.527 $\pm$ 0.033	0.101 $\pm$ 0.011	1.479 $\pm$ 0.488	1.238 $\pm$ 0.397
		0.595 $\pm$ 0.047	0.470 $\pm$ 0.039	0.335 $\pm$ 0.116	1.090 $\pm$ 0.614	0.900 $\pm$ 0.539
40% SiC <sub>p</sub> , 6061 aluminum	177	0.397 $\pm$ 0.033	0.313 $\pm$ 0.027	0.129 $\pm$ 0.016	0.939 $\pm$ 0.217	0.792 $\pm$ 0.184
		0.351 $\pm$ 0.011	0.278 $\pm$ 0.008	0.093 $\pm$ 0.007	1.211 $\pm$ 0.239	1.014 $\pm$ 0.201
		0.268 $\pm$ 0.054	0.211 $\pm$ 0.045	—	0.428 $\pm$ 0.154	0.346 $\pm$ 0.130
55% SiC <sub>p</sub> , 6061 aluminum	283	0.447 $\pm$ 0.038	0.345 $\pm$ 0.026	0.133 $\pm$ 0.018	0.972 $\pm$ 0.253	0.808 $\pm$ 0.216
		0.431 $\pm$ 0.024	0.333 $\pm$ 0.022	0.119 $\pm$ 0.011	1.165 $\pm$ 0.097	0.961 $\pm$ 0.109
		0.268 $\pm$ 0.035	0.206 $\pm$ 0.031	0.105 $\pm$ 0.017	0.558 $\pm$ 0.283	0.463 $\pm$ 0.242

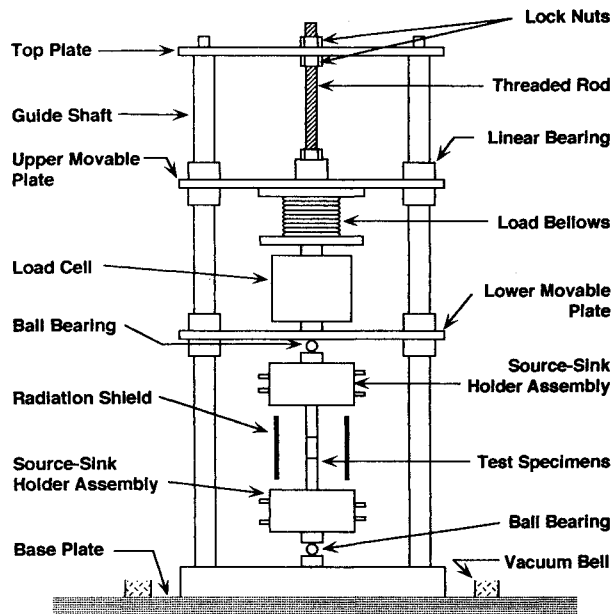


Fig. 1 Experimental test facility (vacuum jar not shown).

## Experimental Program

### Experimental Facility

The experimental apparatus consisted of a roughing pump and oil diffusion pump in series that connected to a 76-cm- (30-in.-) tall metal bell jar to provide a near vacuum environment of less than  $10^{-5}$  torr for the test facility. The test column consisting of the following elements, is shown in Fig. 1. A liquid-cooled copper heat sink was used, and a collar was machined into the bottom of the sink to hold the top heat-flux meter. The coolant was provided by a Forma Scientific, Inc. model 2161 constant temperature bath. A 2.54-cm- (1-in.-) diam cylindrical heat-flux meter was inserted into the collar of the heat sink with thermal grease to insure low contact resistance between the components. The opposite end of the flux meter contacted either an NBS electrolytic iron calibration standard or an MMC test specimen, depending on whether thermal conductivity calibration of the heat-flux meters or thermal conductivity/contact conductance measurements of the MMC were to be performed. If similar metal thermal contact conductance was being measured, a second MMC sample was placed adjacent to the first sample. Next in series was the bottom heat-flux meter held by a collar machined in the bottom heat source fixture. The heat source consisted of a 600-W resistance heater. The actual power dissipation was controlled by varying the input current. A load cell was located above the heat sink directly below a

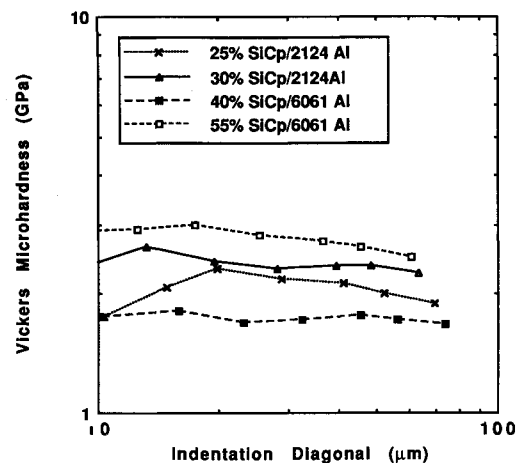


Fig. 2 Vickers microhardness as a function of indentation diagonal for several MMC materials.

bellows system that was used to apply a known force to the test column. Data acquisition was performed with the aid of a Hewlett Packard 3497A data acquisition/control unit connected to a terminal, disk drive, and printer.

### Sample Preparation

The metal matrix composite materials are listed in Table 1. Holes were drilled to the centerline of one 30% SiC<sub>p</sub>/2124 aluminum sample for direct thermal conductivity measurement. A 0.635-cm- (0.25-in.-) resin-bound, diamond-surface grinding wheel was used to grind the remaining sample surfaces to a uniform finish. The fine-grit nib method of truing was used to grind the diamond wheel. A depth feed of 0.0127 mm (0.0005 in.) per whole pass across the surface was used. Two final passes at depth feeds of 0.051 mm (0.0002 in.) were performed as the finish cut. Large depth feeds were not used to avoid applying large pressures (and hence, plastic deformations) to the opposing surface faces that had already been finished and were contacting the steel mounting plate.

Type K thermocouples were fabricated and installed in each hole using a combination of thermal epoxy and aluminum metallic powder. Type K thermocouples have a normal operating range of 73 to 1533 K, (ASTM 470B<sup>11</sup>). Checks were performed to insure that preferential chromium vaporization did not alter the thermocouples' characteristics over time. This problem can be encountered when operating under vacuum conditions for extended periods of time. Standard thermocouple-anchoring techniques were employed.<sup>12</sup>

### Microhardness Measurements

The Vickers microhardness of one sample of each material type was tested at room temperature using a Micromet au-

tomatic microhardness tester. Indentation loads of 10, 25, 50, 100, 200, 300, and 500 g were used on each sample surface. Each load was applied for 15 s. Since the MMC materials are anisotropic at the scale of the lower indentation sizes, five measurements were taken at each load and an average value calculated. The results are shown in Fig. 2 as Vickers microhardness as a function of indentation diagonal.

#### Surface Topography Measurements

Due to the anisotropic nature of the ground specimens, surface characterization consisted of profilometer measurements at 0, 45, and 90 deg to the lay along the centerline. Sampling length was 20 mm (0.787 in.). Measurements were taken with a Surfanalyzer 5000/400 made by Federal Products Corporation. Each sample, as well as the profiling hardware, rested on a granite block that dampened external vibrations that would otherwise introduce measurement errors. The measurement area was also free of air gusts that would adversely affect the results. The topography data was used primarily for nondimensionalization of the contact conductance using rms minimum and maximum surface slope and roughness.<sup>5,9</sup> Other parameters were measured and archived since there remains little consensus as to which surface parameters are actually needed to characterize contact conductance. For example, a model developed by Greenwood and Williamson and modified by McWaid and Marshall,<sup>13</sup> uses moments of the profile power spectral density to predict thermal contact resistance. These moments, along with many other parameters such as arithmetic and rms waviness, have been measured.

Average surface measurements along with standard deviations are shown in Table 1 for the different MMC materials. Figures 3 and 4 show the degrees to which the assumption of a bivariate normal distribution will describe the directional variation of surface slope. The distribution is a basic assumption for using the theory of DeVaal et al.<sup>5</sup>

#### Heat-Flux Meter Calibration

The two heat-flux meters consisted of 6061-T6 aluminum alloy cylinders 2.54 cm (1.00 in.) in diameter with four thermocouples placed at intervals along the centerline. The heat-flux meters were calibrated using an electrolytic iron standard from NIST/NBS, which also contained its own set of thermocouples along the centerline. A steady-state heat-flux was established in the test stack prior to measuring the thermal conductivity of the flux meters. Steady state was defined to be the point at which all thermocouples had less than 0.5 K/h temperature change. The reduced calibration data is shown in Fig. 5 as heat-flux meter thermal conductivity versus temperature. This data was necessary for determining the axial heat-flux through the meters during testing for MMC contact conductance and thermal conductivity.

#### Experimental Test Procedure

One sample (2124 Al/30% SiC<sub>p</sub>) was instrumented with five thermocouples and tested for thermal conductivity in the standard fashion using measured temperature gradients through the sample. Contact conductance tests were performed at mean interface temperatures of 273 K (32 F), 298 K (77 F), and 373 K (212 F), and apparent contact pressures of 1.3 MPa (190 psi), 1.7 MPa (250 psi), 2.6 MPa (380 psi), 3.5 MPa (510 psi), 4.3 MPa (620 psi), 5.2 MPa (750 psi), and 7.0 MPa (1020 psi). Each sample combination was placed between the two flux meters with aligned maximum surface slope. The load was adjusted to the correct apparent contact pressure after the chamber had been evacuated. Data were taken after all temperatures reached steady state, as previously defined. One repeatability test was performed for the 2124 Al/30% vol. SiC particulate samples at a mean interface temperature of 298 K (77 F) and 373 K (212 F) and apparent contact pressures as listed above. Overall conductance was calculated by finding the axial heat-flux through the samples using the heat-flux

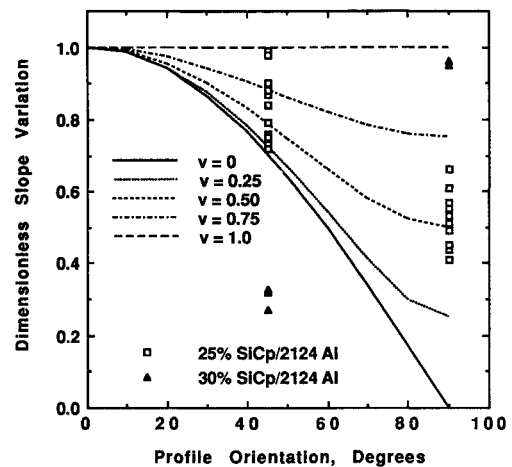


Fig. 3 Comparison of the bivariate-normal slope distribution and experimental data for 25 and 30% SiC<sub>p</sub> with 2124 aluminum.

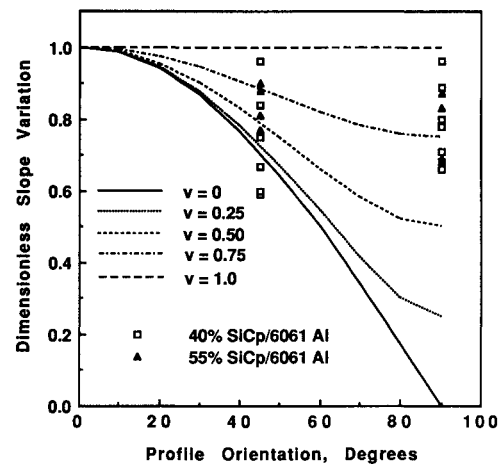


Fig. 4 Comparison of the bivariate-normal slope distribution and experimental data for 40 and 55% SiC<sub>p</sub> with 6061 aluminum.

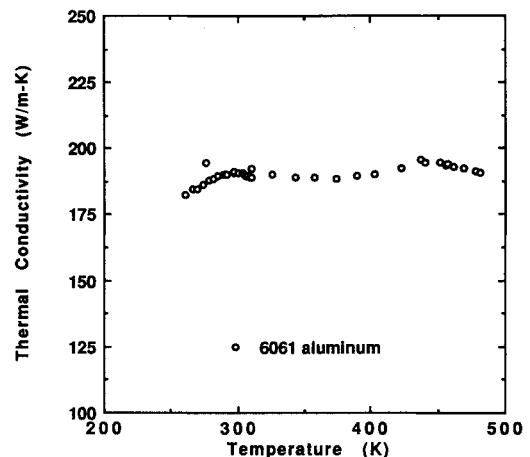


Fig. 5 Thermal conductivity as a function of temperature for 6061 aluminum flux meter calibration data.

meters and determining the temperature jump across the samples by extrapolating thermocouple temperature data from each heat-flux meter to the heat-flux meter edge.

#### Uncertainty Analysis

A number of factors contribute to the uncertainty of the experimental results, particularly the errors in the temperature measurements due to the limit of accuracy of the thermocouple wire, as well as the signal noise in the instrumentation, and the uncertainties in the material thermal conduc-

tivity. Based on a calibration of the aluminum 6061-T6 heat-flux meters, the uncertainty in the thermal conductivity was estimated to be 3.1%. The special limit-of-error grade thermocouple wire is  $\pm 1.1^\circ\text{C}$  ( $\pm 2^\circ\text{F}$ ). With these errors, an estimate of the uncertainty in the thermal contact conductance was made using the method of Kline and McClintock.<sup>14</sup> The uncertainty in the thermal contact conductance was estimated to range from 5.9 to 8.6%.

### Results and Discussion

Figure 6 shows the thermal conductivity as a function of temperature for 30% SiC<sub>p</sub>/2124 aluminum. Mohn and Vukobratovich<sup>6</sup> reported a value of 123 W/m-K. Mil-Hdbk-5E<sup>15</sup> reports a room temperature value of 150.5 W/m-K for 2124 aluminum alloy. Touloukian et al.<sup>16</sup> report wide variations in room temperature SiC thermal conductivity, depending on the form (single crystal, polycrystalline, hot pressed, frit-bonded, etc.). A back-calculation of the MMC SiC thermal conductivity using a simple rule of mixtures yields a thermal conductivity of 122 W/m-K.

Figures 7–10 show the contact conductance vs apparent contact pressure for the four MMC materials tested. Note that all of these figures represent dissimilar junction material values in that the contact is formed by one MMC surface in contact with a flux meter 6061-T6 aluminum surface. Each individual contact conductance value was calculated as the average of both dissimilar-metal contact junctions formed when the MMC sample was placed between the two flux meters. Figure 7 depicts the temperature dependence of contact conductance for 55% SiC<sub>p</sub>/6061 aluminum. Data at three differ-

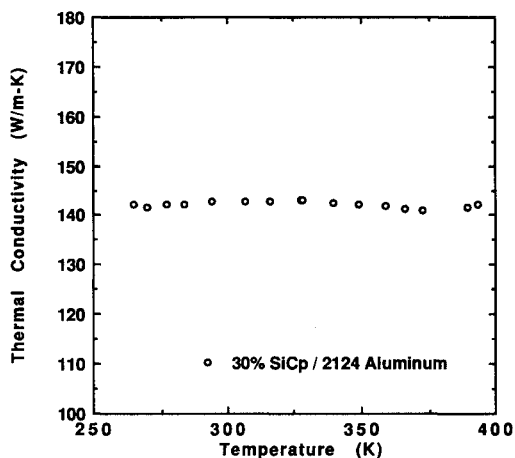


Fig. 6 Thermal conductivity as a function of temperature for 30% SiC<sub>p</sub> with 2124 aluminum.

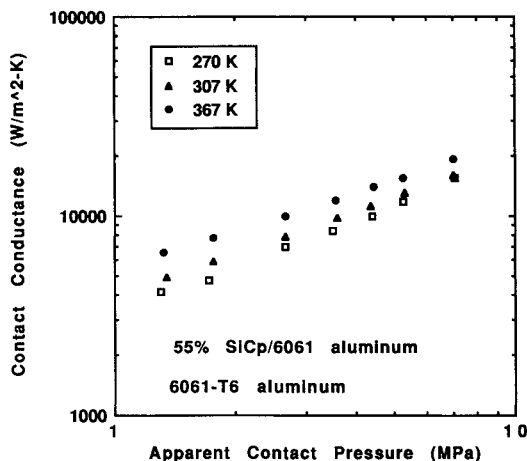


Fig. 7 Contact conductance as a function of apparent pressure (side A, 55% SiC<sub>p</sub> with 6061 aluminum; side B, 6061-T6 aluminum).

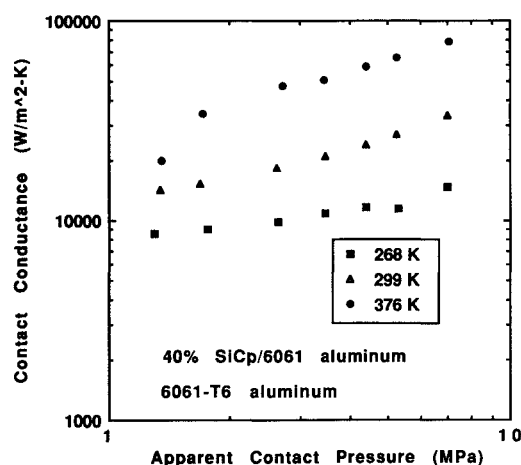


Fig. 8 Contact conductance as a function of apparent pressure (side A, 40% SiC<sub>p</sub> with 6061 aluminum; side B, 6061-T6 aluminum).

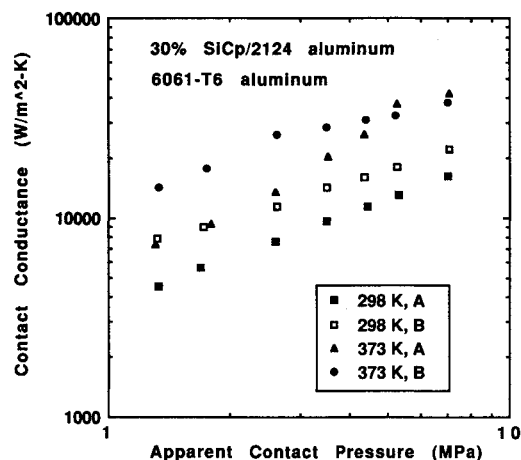


Fig. 9 Contact conductance as a function of apparent pressure (side A, 30% SiC<sub>p</sub> with 2124 aluminum; side B, 6061-T6 aluminum).

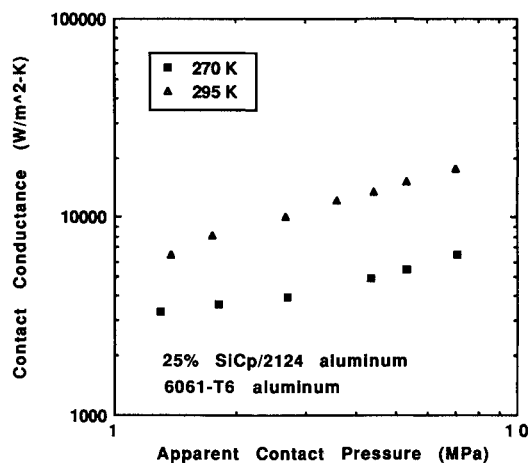


Fig. 10 Contact conductance as a function of apparent pressure (side A, 25% SiC<sub>p</sub> with 2124 aluminum; side B, 6061-T6 aluminum).

ent temperatures are shown, and the expected trend of increasing conductance with increasing interface temperature is clearly seen. The data also appear to be tending towards an asymptote at higher apparent contact pressures, as expected. Figure 8 displays the same trends, but for 40% SiC<sub>p</sub>/6061 aluminum MMC. Figure 9 shows data for two separate samples at two temperatures. If the surface-finish parameters of the two 30% SiC<sub>p</sub>/2124 aluminum MMC samples were exactly the same, near-perfect agreement between the two data sets

would be expected. However, the measured surface profiles indicate differences, and indeed this is what the data show. Figure 10 shows the contact conductance data for the 25% SiC<sub>p</sub>/2124 aluminum MMC. The trends are again in the anticipated direction.

Similar junction contact conductance data between two MMC surfaces are shown in Figs. 11 and 12, as derived from the

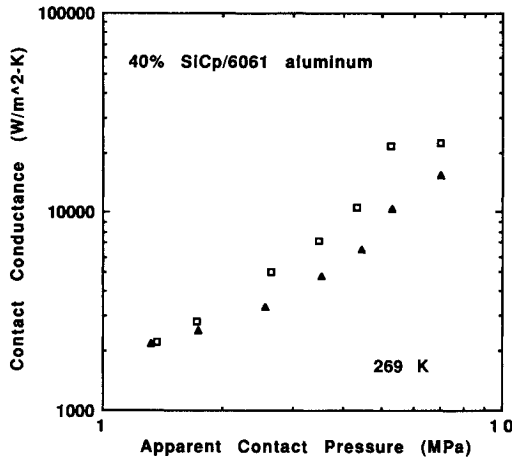


Fig. 11 Contact conductance as a function of apparent pressure (sides A and B, 40% SiC<sub>p</sub> with 6061 aluminum; mean interface temperature, 269 K).

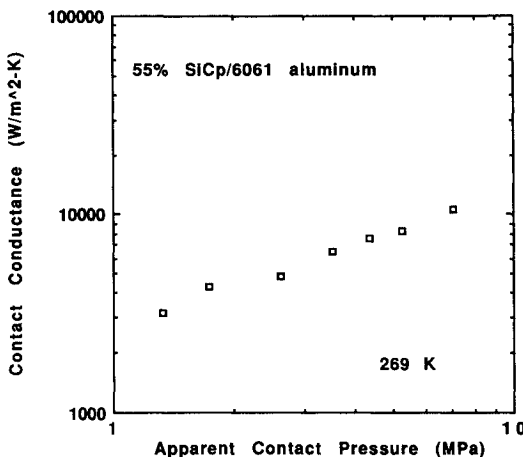


Fig. 12 Contact conductance as a function of apparent pressure (sides A and B, 55% SiC<sub>p</sub> with 6061 aluminum; mean interface temperature, 269 K).

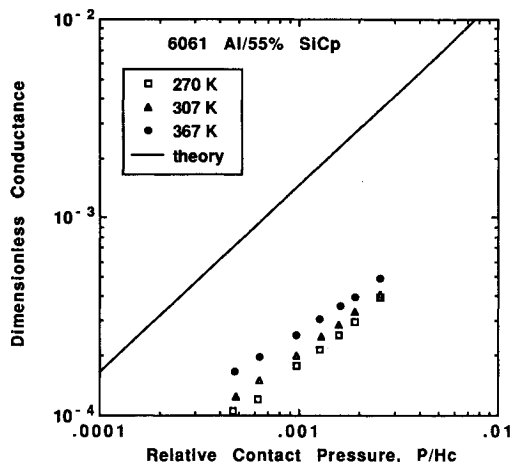


Fig. 13 Comparison between theory and experimental data (6061 aluminum with 55% SiC<sub>p</sub>).

data. Figure 11 is for 40% SiC<sub>p</sub>/6061 aluminum MMC, and Fig. 12 is for 55% SiC<sub>p</sub>/6061 aluminum MMC. These data are for the single interface temperature of 269 K (25 F) and were derived from overall conductance data taken for a stack of two samples between the heat-flux meters. The data reduction procedures therefore required estimates of the flux meter to MMC contact conductance. The recommended procedure for obtaining MMC to MMC contact conductance would be to make measurements with a single interface of two MMC samples that have embedded thermocouples for measuring heat-flux. This was not done because of the significant difficulty of drilling thermocouple holes in the MMC materials. In retrospect, the measurements might have been made by applying the thermocouples to the outside of the MMC cylindrical samples and assuming that the resulting temperature distribution in the samples was one dimensional.

Figures 13–16 show the nondimensionalized data compared with the theory of DeVaal et al.<sup>5</sup> Figure 13 shows the dimensionless conductance vs relative contact pressure for the 55% SiC<sub>p</sub> MMC material. The contact microhardness value used to nondimensionalize the apparent contact pressure was simply an arithmetic average of each set of 35 measurements for each material. This was justified because of the limited variation in Vickers microhardness over the measured indentation diagonal range. In Figs. 13–16, the data fall well below the theoretical predictions. This may be due to the fact that the samples do not follow the bivariate normal probability density function for surface slope with direction that is assumed in the theory. Also, the theory was not meant to account for the increase in constriction resistance due to composite particles interrupting the normal flux tube heat line

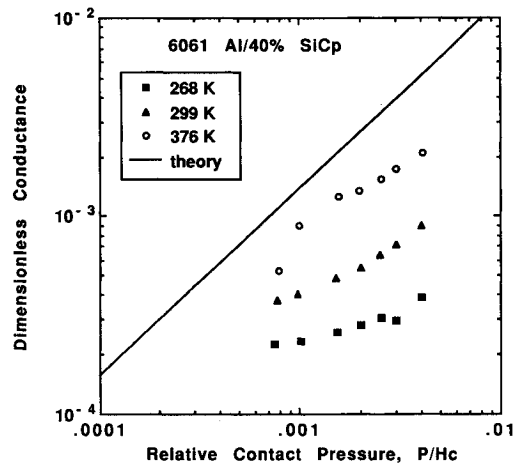


Fig. 14 Comparison between theory and experimental data (6061 aluminum with 40% SiC<sub>p</sub>).

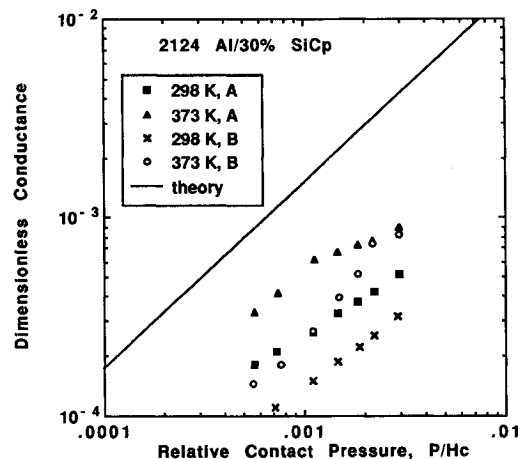


Fig. 15 Comparison between theory and experimental data (2124 aluminum with 30% SiC<sub>p</sub>).

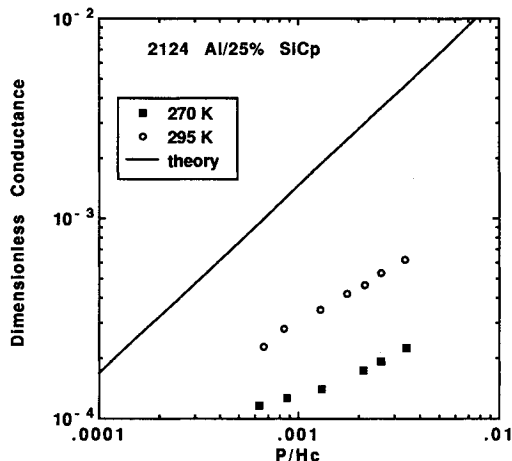


Fig. 16 Comparison between theory and experimental data (2124 aluminum with 25% SiC<sub>p</sub>).

distribution. This suggests that perhaps a theoretical model is needed for a basic flux tube that includes effects of composite particles on constriction resistance. To apply such a model to a realistic material would require a knowledge of the average contact area and how this compares with the average particle size. The material could be treated as isotropic with constant thermal properties if the composite particle size were small in comparison with the flux tube size. Otherwise, the anisotropic effects on constriction resistance would be required. The data also indicate that theoretical models may be desirable in the future that account for surface slope distributions other than bivariate normal.

### Conclusions

Thermal contact conductance data has been presented for aluminum alloy matrix composites with different volumetric loading fractions of particulate silicon carbide. The measurements included results over an interface temperature range of 268–376 K. Dimensionless contact conductance data are presented as a function of relative contact pressure for comparison with the theory of DeVaal et al.<sup>5</sup> The MMC materials included the effects of anisotropy at the scale of the contacts due to the nature of the composite, and this effect was not included in the DeVaal et al.<sup>5</sup> model. Also, the surface slope distributions were not characterized by the bivariate normal probability density function inherent to the DeVaal model. This suggests that the development of new theoretical models to account for these effects may be desirable.

### Acknowledgments

This work was sponsored in part by NSWC Contract N00164-91-C-0043 and the Center for Space Power at Texas A&M

University. The metal matrix composite samples were provided by DWA Composites Specialties, Inc.

### References

- <sup>1</sup>Fletcher, L. S., "Recent Developments in Contact Conductance Heat Transfer," *Journal of Heat Transfer*, Vol. 110, No. 4(B), 1988, pp. 1059–1070.
- <sup>2</sup>Rhoades, M., and Moses, W. M., "Thermal Contact Conductance Between Aligned, Unidirectional Carbon/Epoxy Resin Composites," AIAA Paper 90-0540, Jan. 1990.
- <sup>3</sup>Rhoades, M., and Moses, W., "Thermal Contact Conductance Between Aligned, Unidirectional Carbon/Epoxy Resin Composites Under Vacuum Conditions," AIAA Paper 91-0379, Jan. 1991.
- <sup>4</sup>Rhoades, M. E., "An Experimental Investigation of Thermal Contact Conductance Across Carbon/Fiber/Epoxy Resin Composites as a Function of Interface Pressure," M.S. Thesis, Mechanical Engineering Dept., Texas A&M Univ., College Station, TX, Dec. 1989.
- <sup>5</sup>DeVaai, J. W., Yovanovich, M. M., and Negus, K. J., "The Effects of Surface Slope Anisotropy on the Contact Conductance of Conforming Rough Surfaces," *Fundamentals of Conduction and Recent Development in Contact Resistance*, edited by M. Imber, G. P. Peterson, and M. M. Yovanovich, American Society of Mechanical Engineers HTD-Vol. 69, 1987, pp. 123–134.
- <sup>6</sup>Mohn, W. R., and Vukobratovich, D., "Recent Applications of Metal-Matrix Composites in Precision Instruments and Optical Systems," *Optical Engineering*, Vol. 27, No. 2, 1988, pp. 90–98.
- <sup>7</sup>Rubin, L., "Applications of Metal-Matrix Composites, the Emerging Structural Materials," *SAMPE Journal*, Vol. 15, No. 4, 1979, pp. 4–10.
- <sup>8</sup>Kinner, W. K., "Metal-Matrix Composites," *Materials Engineering*, Vol. 91, No. 1, 1980, pp. 64–66.
- <sup>9</sup>Yovanovich, M. M., and Nho, K., "Experimental Investigation of Heat Flow Rate and Direction on Contact Resistance of Ground/Lapped Stainless Steel Interfaces," AIAA Paper 89-1657, June 1989.
- <sup>10</sup>Cooper, M. G., Mikic, B. B., and Yovanovich, M. M., "Thermal Contact Conductance," *International Journal of Heat and Mass Transfer*, Vol. 12, No. 1, 1969, pp. 279–300.
- <sup>11</sup>*Manual on the Use of Thermocouples in Temperature Measurement*, American Society for Testing and Materials, STP 470B, Philadelphia, PA, 1981.
- <sup>12</sup>Hust, J. G., "Thermal Anchoring of Wires in Cryogenic Apparatus," *Review of Scientific Instruments*, Vol. 41, No. 5, 1970, pp. 622–624.
- <sup>13</sup>McWaid, T., and Marschall, E., "Predicting the Thermal Contact Resistance Across Pressed Metal Contacts in a Vacuum Environment," *Experimental/Numerical Heat Transfer in Combustion and Phase Change*, HTD-Vol. 170, July 1991, pp. 17–23.
- <sup>14</sup>Kline, S. J., and McClintock, F. A., "Describing Uncertainties in Single-Sample Experiments," *Mechanical Engineering*, Vol. 75, No. 1, 1953, pp. 3–8.
- <sup>15</sup>*Metallic Materials and Elements for Aerospace Vehicle Structures*, Dept. of Defense, MIL-HDBK-5E, Philadelphia, PA, 1987.
- <sup>16</sup>Touloukian, Y. S., Powell, R. W., Ho, C. Y., and Clemens, P. G., *Thermophysical Properties of Matter, Vol. 1, Metallic Elements and Alloys*, TPRC Purdue Univ., Plenum, New York, 1970, pp. 585–588.